Acta Oceanol. Sin., 2025, Vol. 44, No. 1, P. 17–27
https://doi.org/10.1007/s13131-024-2440-6

Modulation of marine heatwaves by salinity effect in the Northeast Pacific Ocean in 2013–2014

Xiaokun Wang[1, 2], Hai Zhi[1*], Ronghua Zhang[3, 4], Jiaxiang Gao[3, 5], Pengfei Lin[6]

[1] School of Atmospheric Sciences, Nanjing University of Information Science and Technology, Nanjing 210044, China

[2] Henan Meteorological Disaster Prevention Technology Center, Zhengzhou 450003, China

[3] School of Marine Sciences, Nanjing University of Information Science and Technology, Nanjing 210044, China

[4] Laoshan Laboratory, Qingdao 266237, China

[5] Jiangsu Key Laboratory of Atmospheric Environment Monitoring and Pollution Control, Collaborative Innovation Center of Atmospheric Environment and Equipment Technology, School of Environmental Science and Engineering, Nanjing University of Information Science and Technology, Nanjing 210044, China

[6] State Key Laboratory of Numerical Modeling for Atmospheric Sciences and Geophysical Fluid Dynamics, Institute of Atmospheric Physics, Chinese Academy of Sciences, Beijing 100029, China

Received 19 August 2024; accepted 7 December 2024

Abstract

Marine heatwaves (MHWs) are extreme ocean events characterized by anomalously warm upper-ocean temperatures, posing significant threats to marine ecosystems. While various factors driving MHWs have been extensively studied, the role of ocean salinity remains poorly understood. This study investigates the influence of salinity on the major 2013–2014 MHW event in the Northeast Pacific using reanalysis data and climate model outputs. Our results show that salinity variabilities are crucial for the development of the MHW event. Notably, a significant negative correlation exists between sea surface temperature anomalies (SSTAs) and sea surface salinity anomalies (SSSAs) during the MHW, with the SSSAs emerging simultaneously with SSTAs in the same area. Negative salinity anomalies (SAs) result in a shallower mixed layer, which suppresses vertical mixing and thus sustains the upper-ocean warming. Moreover, salinity has a greater impact on mixed layer depth anomalies than temperature. Model sensitivity experiments further demonstrate that negative SAs during MHWs amplify positive SSTAs by enhancing upper-ocean stratification, intensifying the MHW. Additionally, our analysis indicates that the SAs are predominantly driven by local freshwater flux anomalies, which are mainly induced by positive precipitation anomalies during the MHW event.

Key words marine heatwave, salinity effect, ocean stratification and mixing, sea surface temperature, Northeast Pacific Ocean

Citation Wang Xiaokun, Zhi Hai, Zhang Ronghua, Gao Jiaxiang, Lin Pengfei. 2025. Modulation of marine heatwaves by salinity effect in the Northeast Pacific Ocean in 2013–2014. Acta Oceanologica Sinica, 44(1): 17–27, doi: 10.1007/s13131-024-2440-6

1 Introduction

Marine heatwaves (MHWs), defined as prolonged periods of anomalously high sea surface temperature (SST), were first defined following an unusual ocean warming event off the western coast of Australia in 2010/2011 by Pearce et al. (Pearce et al., 2011). MHWs exert considerable ecological and socio-economic impacts, including shifts in marine species distribution, local extinctions, and significant damage to seafood industries (Kintisch, 2015;

Foundation item: The Laoshan Laboratory under contract Nos LSKJ202202403 and LSKJ202202402; the National Natural Science Foundation of China under contract Nos 42030410 and 42406202; the Natural Science Foundation of Jiangsu Province under contract No. BK20240718; the Startup Foundation for Introducing Talent of Nanjing University of Information Science and Technology; the Jiangsu Innovation Research Group under contract No. JSSCTD202346; the Jiangsu Funding Program for Excellent Postdoctoral Talent under contract No. 2023ZB690.

*Corresponding author, E-mail: zhihai@nuist.edu.cn

Cavole et al., 2016; Hobday et al., 2016; Viglione, 2021). Throughout the 21st century, the frequency, duration, and intensity of MHWs worldwide are projected to increase significantly under global warming (Oliver et al., 2017, 2018; Cheng et al., 2023), leading to greater harm to marine ecosystems and more substantial socio-economic impacts. Hence, understanding the physical mechanisms driving MHW occurrence and development is essential for improving predictions of these events and mitigating their impacts (Hu et al., 2017; Holbrook et al., 2019; Gupta et al., 2020; Zhang et al., 2020; Wang et al., 2021).

In recent years, the Northeast Pacific has experienced severe and widespread MHWs. Specifically, significant MHWs occurred during the winter of 2013–2014 and the summer of 2019 (Bond et al., 2015; Amaya et al., 2020; Song et al., 2023). The 2013–2014 MHW event had devastating effects on phytoplankton growth due to the persistent presence of warm, nutrient-poor waters (Bond et al., 2015; Kintisch, 2015). This event triggered cascading ecological impacts, including a sharp decline in the Chinook salmon population and the distressing loss of up to one million seabirds near the Gulf of Alaska (Smale et al., 2019). Meanwhile, the prolonged heat, combined with unusually weak coastal winds, disrupted upwelling along much of the Pacific coast, leading to atmospheric rivers being blocked by a persistent ridge of high pressure over the North Pacific from 2012 to 2015 (Chen et al., 2023). These catastrophic consequences highlight the urgency of investigating the causes of MHWs in the Northeast Pacific.

The driving mechanisms of MHWs are very complex. Holbrook et al. (2019) examined the formation mechanisms of MHWs across various ocean regions and found substantial variations in the processes involved. In general, MHWs are driven by the combined effects of internal climate variability and external forcing from human activities (Hu and Li, 2022). Previous studies have identified three primary mechanisms contributing to MHW formation. (1) Atmospheric forcings, such as increased solar radiation, sensible and latent heat fluxes, and wind stress can drive MHWs (Wang et al., 2021; Holbrook et al., 2020). (2) Oceanic dynamic processes play an important role in the formation of MHWs, especially in the development of subsurface MHWs. Key processes include the strengthening of warm advection, shoaling of the mixed layer, enhanced oceanic stratification, weakened vertical mixing, reduced upwelling, and suppressed Ekman suction (Oliver et al., 2021; Holbrook et al., 2019; Miao et al., 2021). (3) Large-scale climate models such as El Niño-Southern Oscillation (ENSO), Madden-Julian Oscillation (MJO), Pacific Decadal Oscillation (PDO), and North Atlantic Oscillation (NAO) can significantly influence MHW formation through atmospheric forcing or teleconnection (Scannell et al., 2016).

Salinity is a fundamental ocean state variable that plays a vital role in oceanic physical processes. Previous studies have shown that salinity significantly influences various processes by directly affecting seawater density, which in turn impacts upper-ocean stratification and mixed layer depth (MLD) (Miller, 1976; Lukas and Lindstrom, 1991; Manabe and Stouffer, 1995; Oka and Hasumi, 2004; Delcroix et al., 2007; Bosc et al., 2009; Zhang and Busalacchi, 2009). For instance, Zhu et al. (2014) performed two forecast experiments to explore the impact of salinity interannual variability on ocean initial state, which highlights the indispensable role of salinity variability in accurately identifying and understanding extreme climatic events in the ocean. Zheng and Zhang (2015) further emphasized that interannual variations in salinity contribute more significantly to density and mixed layer-related stratification than temperature, underlining its importance. Furthermore, ocean stratification associated with salinity changes contributes significantly to maintaining the heat balance of the upper ocean at both seasonal and interannual variabilities (Zhang et al., 2010, 2012; Jouanno et al., 2011; Vinogradova and Ponte, 2013). Low-salinity water promotes strong stratification, inhibiting vertical mixing processes (Sprintall and Tomczak, 1992). Positive anomalies in barrier layer thickness prevent cooler, saltier water from mixing into the upper layer, leading to increased SST (Maes et al., 2005; Da-Allada et al., 2014; Hu and Sprintall, 2016). Consequently, decreases (increases) in salinity result in a shallower (deeper) mixed layer, causing SSTs to warm (cool) (Zheng et al., 2014; Zhi et al., 2015, 2019b; Shi et al., 2022).

The relationship between salinity and MLD suggests that salinity variations can significantly influence the development of MHWs. A previous study found that decreased salinity in the mixed layer causes more stable stratification, reducing the entrainment of subsurface cold water into the mixed layer (Li and Zheng, 2022). This process allows anomalous heat to accumulate in the mixed layer, thereby increasing the likelihood of MHWs. Scannell et al. (2020) compared two recent MHWs in the Northeast Pacific using observational data and found that salinity plays an essential role in their development by modifying ocean stability. While these studies have highlighted the importance of salinity in MHW development, several key questions remain unanswered. For example, what are the driving factors behind salinity anomalies (SAs) during the formation of MHWs? How do SAs contribute to upper-ocean stratification changes in association with MHWs?

In this study, we aim to explore the relationship between sea surface salinity anomalies (SSSAs) and MHWs, quantify the contribution of salinity changes to MHW development, and identify the sources of salinity changes. We focus on the 2013–2014 MHW event in the Northeast Pacific using both reanalysis data and climate model outputs. The remainder of this paper is organized as follows. Data and methods are introduced in Section 2. Section 3 presents our major findings about the role of SSSAs in upper-ocean stratification during the MHW event. Finally, conclusions and discussion are given in Section 4.

2 Data, methods, and experiment

2.1 *Data*

We use the Optimal Interpolation Sea Surface Temperature (OISST) data from the National Oceanic and Atmospheric Administration to identify observational features of MHWs, including their onset and end dates and cumulative intensity. The OISST data incorporate observations from various instruments (satellites, ships, and buoys) into a regular global grid (Reynolds et al., 2007; Huang et al., 2021). We use daily OISST data from 1992 to 2021 with a horizontal resolution of 0.25° × 0.25° in this study.

To examine the subsurface evolution of MHWs, we adopt 3-dimensional ocean temperature and salinity data from the high-resolution version of the Flexible Global Ocean-Atmosphere-Land System (FGOALS-f3-H) (Bao et al., 2020). This model is developed by the Institute of Atmospheric Physics, Chinese Academy of Sciences, and the model experiments are part of the Ocean Model Intercomparison Project (OMIP), an endorsed project by the Coupled Model Intercomparison Project Phase 6 (CMIP6). OMIP conducts global ocean-sea ice coupled simulations with unified external atmospheric forcings and flux calculation schemes (Yu et al., 2019). The FGOALS-f3-H model outputs span the period from 1958 to 2018, with a horizontal resolution of 0.25° × 0.25°, comparable to the OISST data, and 55 vertical layers ranging from 2.5 m to 5 372.0 m. In this study, we analyze outputs from 2009 to 2018, with 28 vertical layers within the 2.5–195.4 m range.

Because the FGOALS-f3-H output does not include precipitation and evaporation data, we incorporate hourly precipitation and evaporation data from the European Centre for Medium-Range Weather Forecasts Reanalysis v5 (ERA5) (Hersbach et al., 2018) to calculate freshwater flux (FWF) anomalies during MHW events. Although these two reanalysis variables may have biases, they provide spatially and temporally consistent fields for our FWF calculation, which is important for diagnosing the impact of FWF anomalies. The ERA5 data have a horizontal resolution of 0.25° × 0.25° and cover the period from 1992 to 2021. The original hourly data are further processed into daily data to maintain consistency with other datasets used in this study. FWF is calculated as precipitation (P) minus evaporation (E), with positive values indicating downward fluxes into the ocean.

Before analysis, we calculate daily anomalies for all variables by subtracting daily climatology from the original data. Specifically, the daily climatology is computed over the periods 1992–2021 for OISST, 2009–2018 for ERA5, and 2009–2018 for model outputs, based on the availability of each dataset. The daily anomalies are then detrended to remove the global warming signal. These detrended anomaly time series are subsequently used for MHW identification and further analyses.

2.2 *Methods*

In this study, we follow the definition of MHWs proposed by Hobday et al. (2016), that is, SST anomalies (SSTAs) exceeding the 90th percentile of daily climatology for at least five days in a given location. For each day of the year, the daily climatology is derived using data within an 11-d window centered on that day, so a total of 330 d (11 d/a × 30 a) are used to calculate the 90th percentile. MHW events separated by two days or less are treated as a single event.

To analyze the evolution of the 2013–2014 MHW event, three-dimensional salinity and temperature fields from the FGOALS-f3-H are used to determine the MLD. The MLD is defined as the depth at which seawater density deviates by a threshold value of $\Delta\rho$ from the density at 10 m depth, where $\Delta\rho$ is the density difference corresponding to a temperature drop of 0.2℃ at 10 m (Kara et al., 2000; de Boyer Montégut et al., 2004). The resultant MLD anomaly time series from 2009 to 2018 are also detrended.

To better quantify the contribution of the salinity effect to the 2013–2014 MHW event, we conduct an analysis to separate the contributions of temperature and salinity to MLD. Specifically, The MLD field, expressed as $F(T, S)$, is a function of temperature (T) and salinity (S), and its interannual variations can be attributed to changes in either or both variables. Following Zheng and Zhang (2012), we calculate MLD anomalies using interannually varying and climatological temperature and salinity fields from 2009 to 2018. The differences between these MLD anomalies quantify the individual contribution of temperature and salinity changes. We then separately assess the relative impacts of temperature and salinity anomalies on MLD variability.

In addition, we conduct a heat budget analysis to investigate the ocean processes influencing mixed layer temperature variability. This approach has been extensively employed in previous studies (Huang and Mehta, 2004; Huang et al., 2005; Guan et al., 2023; Ye et al., 2023). The governing equation for the mixed layer temperature budget is as follows (Zhang et al., 2005).

$$\frac{\partial T}{\partial t} = -\left(u\frac{\partial T}{\partial x} + v\frac{\partial T}{\partial y}\right) - w\frac{\partial T}{\partial z} + \frac{\kappa_h}{H_m}\nabla_h\cdot(H_m\nabla_h T) + \frac{2\kappa_v}{H_m H_2}(T_e - T) + \frac{Q_{\text{net}}}{\rho C_p H_m}, \quad (1)$$

where $\frac{\partial T}{\partial t}$ is the tendency of the mixed layer temperature, $-\left(u\frac{\partial T}{\partial x} + v\frac{\partial T}{\partial y}\right)$ is the horizontal advection term, $-w\frac{\partial T}{\partial z}$ is the vertical advection term, $\frac{\kappa_h}{H_m}\nabla_h\cdot(H_m\nabla_h T)$ is the horizontal diffusion term, $\frac{2\kappa_v}{H_m H_2}(T_e - T)$ is vertical mixing and sub-surface entrainment terms, $\frac{Q_{\text{net}}}{\rho C_p H_m}$ is the net heat flux term. In the following analysis, the horizontal diffusion, vertical mixing and subsurface entrainment terms are

omitted due to their negligible magnitude compared to other terms.

2.3 *Model and experiment*

To validate the potential salinity effect on MHWs, we use the LICOM3 model (Liu et al., 2012) coupled with the Community Ice Code, version 4 (CICE4) (Lin et al., 2020) to perform sensitivity experiments. The model has a horizontal grid resolution of 360 × 218 in the zonal and meridional directions, respectively, with 30 vertical levels. Spherical coordinates are used in the horizontal direction, while η coordinates are used in the vertical direction.

A series of sensitivity experiments are conducted using the LICOM3 model. Initial and boundary conditions are derived from JRA55-do data. The model is first spun up to a climate state using temperature and salinity data from PHC3.0 over a 200-year integration. Subsequently, daily JRA55-do data with interannual variability are used to force the model from 1958 to 2013, yielding the initial state on January 1, 2013. To investigate the impact of FWF on MHWs, we conduct sensitivity experiments by adjusting precipitation levels within the analysis region to 0%, 50%, 100%, and 200% of the observed values, respectively. The experiments are hereafter referred to as fwf_0, fwf_0.5, fwf_ctl, and fwf_2.0.

3 Results

3.1 *SSTAs and SSSAs associated with the 2013–2014 MHW*

We apply the MHW identification procedure to the OISST data in the Northeast Pacific and successfully identify major MHW events from 1992 to 2021 (Fig. 1a). It can be observed from Fig. 1a that the 2013–2014 MHW event stands out as the most significant event in terms of both duration and intensity. Specifically, the 2013–2014 MHW event spans from November 21, 2013, to March 30, 2014, with a cumulative intensity of 226.76℃, a maximum intensity of 2.55℃, and a duration of 130 d. These characteristics are consistent with previous studies (Zhi et al., 2019a; Scannell et al., 2020; Shi et al., 2022).

Figures 1b–d show the average SSTAs during the 2013–2014 MHW event using both the OISST data and FGOALS-f3-H model outputs. The spatial pattern and temporal variations of SSTAs in the FGOALS-f3-H results are highly consistent with the OISST data. The maximum SSTA during this event reaches 2.75℃ in the OISST data and 2.70℃ in the FGOALS-f3-H outputs. These results indicate that the FGOALS-f3-H effectively reproduces the 2013–2014 MHW event in the Northeast Pacific. In the following analyses, we use the FGOALS-f3-H outputs to examine the subsurface evolution of this MHW event and assess the role of salinity.

To gain a detailed understanding of the physical processes associated with the MHW event, results of the mixed-layer heat budget analysis are presented in Fig. 2. It can be seen from Fig. 2a that the temperature tendency on the right-hand side of Eq. (1) is consistent with the tendency calculated from mixed layer temperature. In Fig. 2b, we present the cumulative heat anomalies by integrating the heat budget terms over time to better illustrate the contribution and evolution of each term during the MHW event. The result shows that the anomalous warming is predominantly driven by the surface heat flux term,

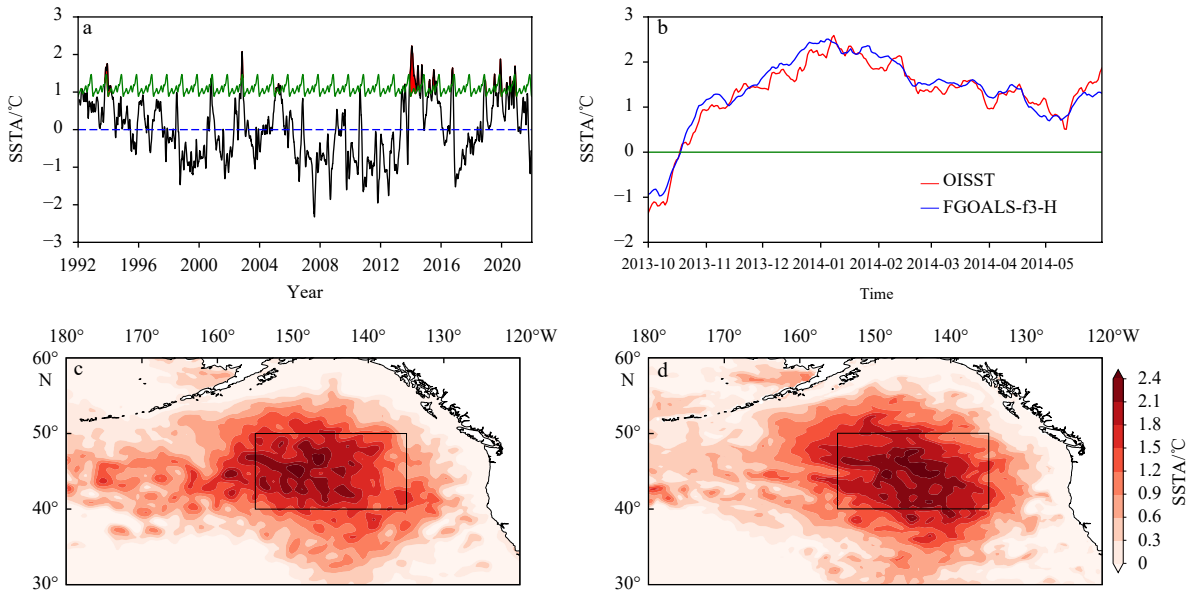

Fig. 1. The 30-day running averaged daily SST from 1992 to 2021 averaged over 40°–50°N, 135°–155°W (black line), with daily MHW threshold (green line). The red-filled area represents MHW events (a). Time series of daily SSTA from October 2013 to May 2014 averaged over 40°–50°N, 135°–155°W from OISST (red) and FGOALS-f3-H (blue) (b). The spatial distributions of mean SSTA from OISST (c) and FGOALS-f3-H (d) during the 2013–2014 MHW (November 21, 2013 to March 30, 2014). The black box represents the region of 40°–50°N, 135°–155°W.

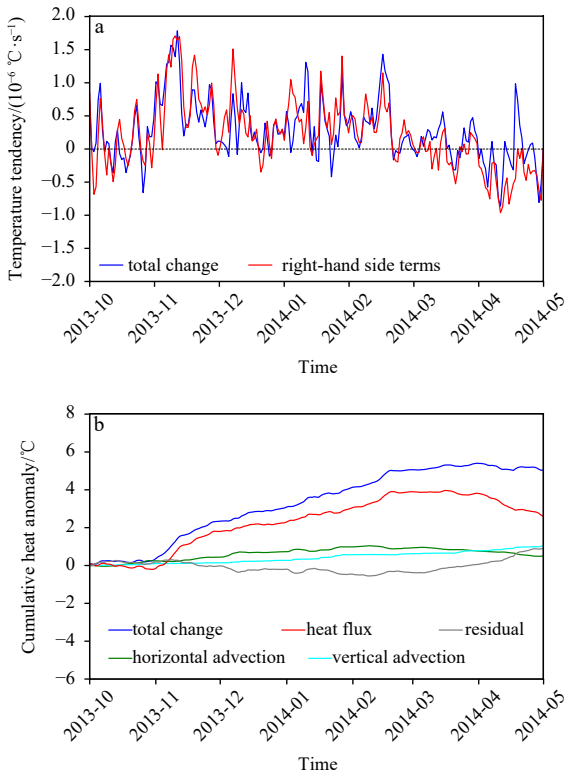

Fig. 2. Time series comparing the sum of right-hand side terms (red) in the heat budget equation with the mixed layer temperature tendency (blue) during the 2013–2014 MHW event (a); cumulative heat anomalies (blue) contributed by the surface heat flux term (red), the vertical advection term (cyan), the horizontal advection term (green), and the residual term (gray) during the MHW event. The heat budget terms are averaged over 40°–50°N, 135°–155°W (b).

as its magnitude is roughly comparable with the total change. In contrast, the horizontal and vertical advection terms contribute significantly less. The residual term remains close to zero during the analysis period, further indicating that the selected terms can well represent the major processes responsible for the anomalous warming. Overall, these results highlight that surface heat flux is the dominant factor driving the upper-ocean warming during this MHW, with limited influence from advection and vertical mixing. This conclusion agrees with previous studies like Chen et al. (2023), indicating the central role of atmospheric anomalies.

The spatial distributions and temporal variations of the SSTAs and SSSAs during the event are displayed in Fig. 3. The positive SSTAs off the west coast of North America coincide well with the negative SSSAs in the same region. Figure 3c shows a strong negative correlation between the time series of SSTAs and SSSAs averaged over 40°–50°N and 135°–155°W, with a correlation coefficient of −0.78. Furthermore, we present the temporal evolutions of SSTAs and SSSAs averaged over the latitudinal range of 40°–50°N in Fig. 4. A prominent positive SSTA center emerges since December 2013, gradually extending eastward as the MHW event progresses. Similarly, a strong negative SSSA center appears in December 2013 and exhibits an eastward extension alongside the SSTA center. These results confirm that the SSTAs and SSSAs develop concurrently in the same region during the MHW event.

3.2 *Salinity-induced stratification anomalies during the MHW*

To better understand the influence of SSSA on the MHW event, the temporal variation of MLD anomalies averaged over 40°–50°N and 135°–155°W is presented in Fig. 5a. Notable MLD anomalies emerge as the MHW event begins to develop. During the early stage of this event (from November 2013 to January 2014), the MLD anomalies remained negative. A shallower mixed layer means that anomalous heat is more likely to accumulate in the upper ocean, leading to stronger MHW intensity (Scannell et al., 2020). After January 2014, the MLD anomalies show alternating positive and negative anomalies, with a gradually increasing amplitude for positive anomalies. This pattern likely contributes to a decrease in positive SSTA, causing the dissipation of the MHW event.

The above analysis qualitatively demonstrates the relationships among SSTA, SSSA, and MLD, emphasizing the crucial role of salinity in influencing SST through its impact on the MLD. However, since the MLD is influenced by both temperature and salinity, it is necessary to separate their individual contributions to the MLD anomalies. To achieve this, we employ the method proposed by Zheng and Zhang (2012) for a quantitative assessment.

We quantify the contributions of SSTA and SSSA to the MLD anomalies during the 2013–2014 MHW event in Figs 5, 6b and 6c. It can be observed that during the early stage of the event, both the SSTA and SSSA contribute to negative MLD anomalies, and the contribution of SSSA is generally greater than that of SSTA. This highlights the important role of SSSA in the onset of the MHW event through its modulation of the MLD. After January 2014, both the SSTA and SSSA contribute to positive MLD anomalies. The timing corresponds to the start of the dissipation stage of the MHW event, so the positive MLD anomalies may facilitate the decline in MHW intensity. It is thus suggested that the modulation effect of salinity is not consistent throughout the event. However, it is not clear what processes cause the shift in the role of SSSA. In this study, we mainly focus on the negative MLD anomalies induced by SSSA during the early stage of the 2013–2014 MHW.

SSSA is typically influenced by surface fluxes, oceanic advection, and subsurface processes, with surface FWF playing a dominant role (Zhang et al., 2006; Hasson et al., 2013). Figure 7a shows the spatial distribution of the average FWF anomalies during the 2013–2014 MHW event.

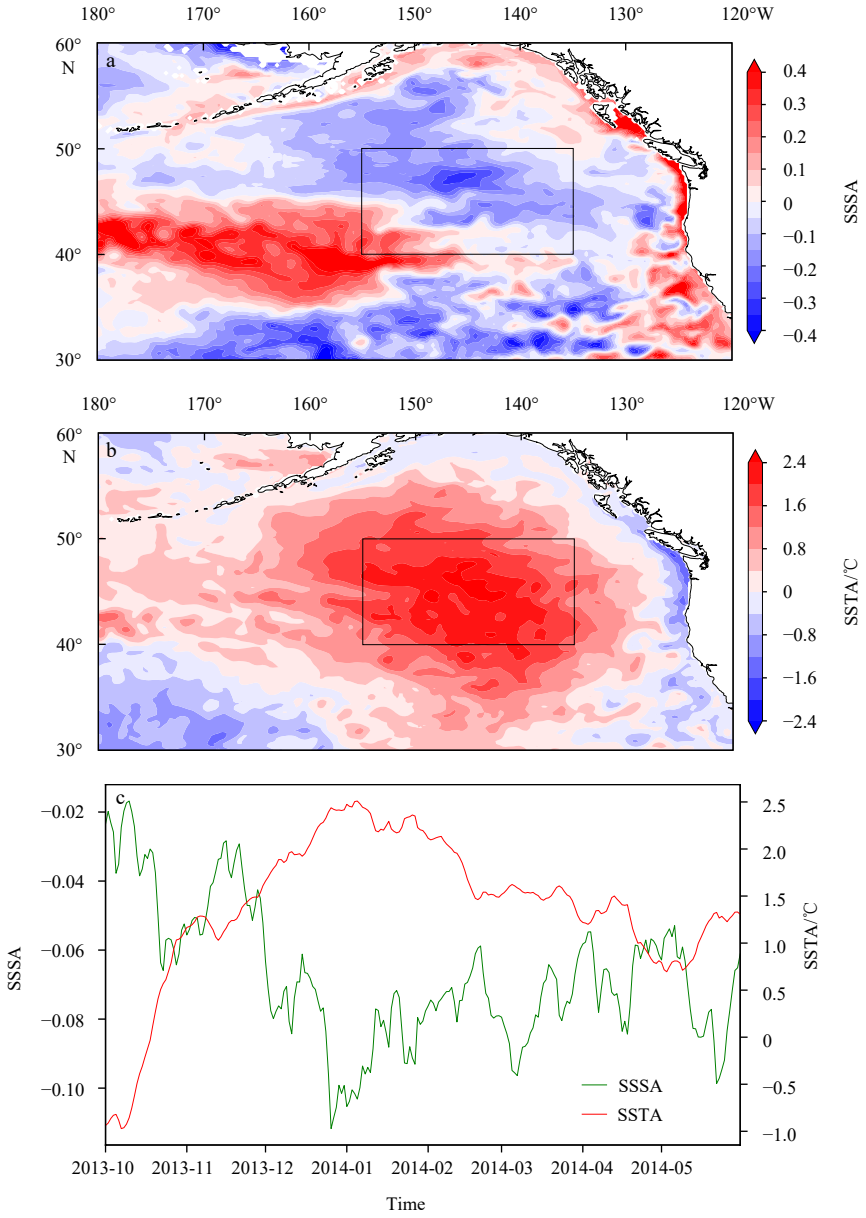

Fig. 3. Spatial distributions of mean SSSAs (a) and SSTAs (b) during the 2013–2014 MHW (November 21, 2013 to March 30, 2014) and time series of daily SSTA (red) and SSSA (green) (c) averaged over 40°–50°N, 135°–155°W derived from FGOALS-f3-H output. The black box represents the region of 40°–50°N, 135°–155°W.

Remarkable positive FWF anomalies can be observed in the same region as the negative SSSA, indicating that an influx of freshwater into the ocean reduces salinity. In Fig. 7b, the peaks in FWF anomalies from November 2013 to January 2014 generally correspond to the dips in both SSSA and MLD anomalies (Figs 3c and 5a). These results show that the negative SSSA observed during the MHW event is likely induced by the positive FWF anomalies.

3.3 *Results from sensitivity experiments*

In order to verify the processes by which FWF anomalies affect the MHW intensity, we use LICOM3 to examine the SSTAs during the 2013–2014 MHW under varying FWF conditions. Figure 8a presents the time series of mean sea surface salinity (SSS) for each experiment, which exhibit considerable differences under varying FWF forcings, highlighting the significant influence of FWF on SSS. In the fwf_ctl experiment, SSS stabilizes at an equilibrium value of 32.2. As the FWF increases, regional SSS decreases since December 2013. Specifically, the fwf_2.0 (a doubled FWF) experiment shows a freshening of salinity 0.5 in comparison to fwf_ctl. The SSS variations significantly impact ocean stratification, as the MLD increases (decreases) in response to higher (lower) SSS (Fig. 8b), indicating a positive correlation between SSSA and MLD anomalies. Notably, the MLD differences between fwf_0 (no FWF) and fwf_2.0 can reach up to 15 m. Corresponding to the MLD changes, the SST demonstrates varying evolutionary features across different experiments, with stronger (weaker) warming observed under increased (decreased) FWF.

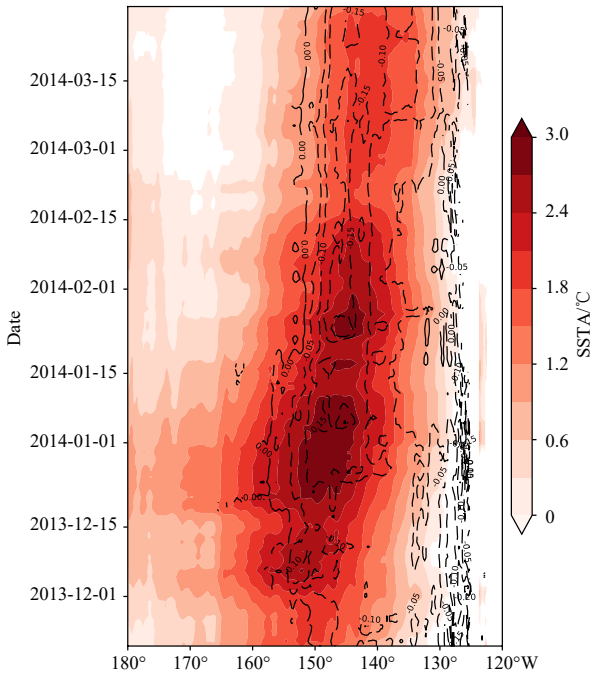

Fig. 4. Time-longitude section of daily SSSAs (contour) and SSTAs (color) averaged over 40°–50°N during the 2013–2014 MHW (November 21, 2013 to March 30, 2014) derived from FGOALS-f3-H output.

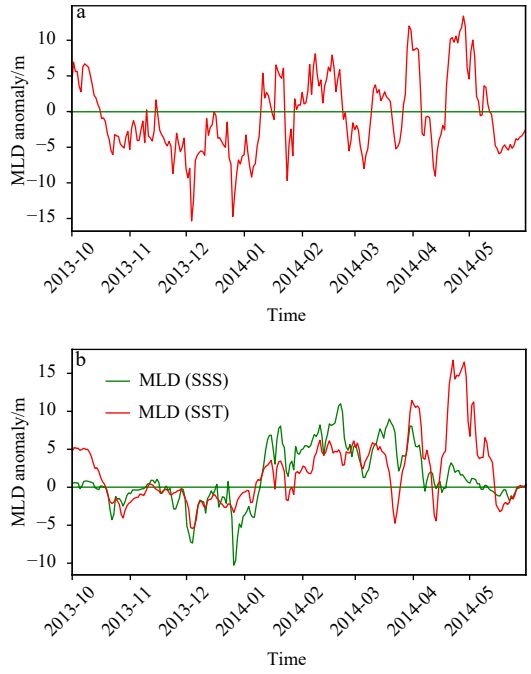

Fig. 5. Time series of daily MLD (a) , MLD (SSS, green) and MLD (SST, red) (b) anomalies averaged over 40°–50°N, 135°–155°W from October 1, 2013, to May 31, 2014 derived from FGOALS-f3-H outputs.

It is worth noting that the MLD and SST responses in the experiments are more pronounced after January 2014, which is not quite consistent with the observations presented above. This delayed response in the model is likely due to the time required for the MLD and SST to adjust to FWF forcing in LICOM3, leading to a more substantial effect during the later stages of the event.

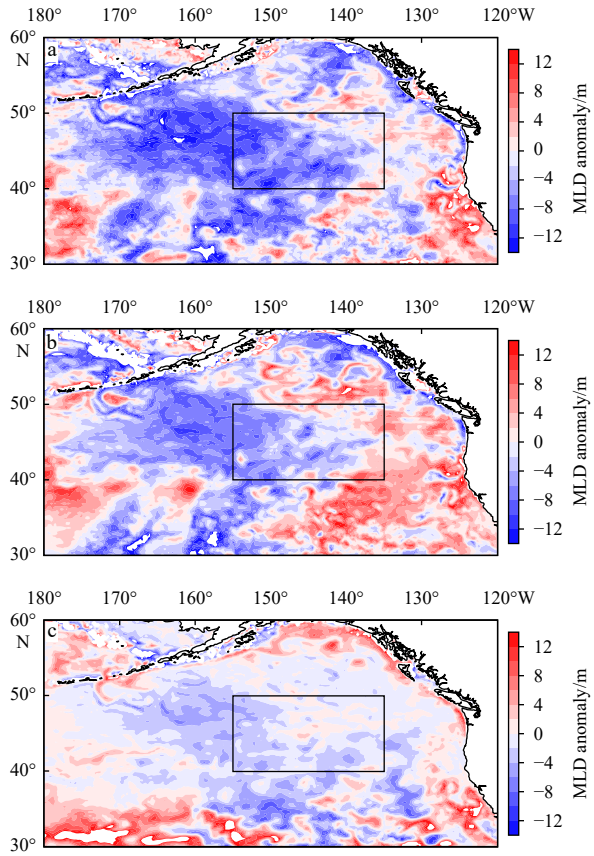

Fig. 6. Spatial distributions of mean MLD anomaly (a) and the contributions of SSSA (b) and SSTA (c) to the MLD anomaly during the early stage of the MHW (November 21, 2013 to June 10, 2014) derived from FGOALS-f3-H output. The black box represents the region of 40°–50°N, 135°–155°W.

In summary, the model sensitivity experiments confirm the close connection among FWF anomalies (i.e., precipitation changes), SSS changes, and the MHW intensity. Specifically, positive FWF anomalies reduce SSS, leading to mixed layer shoaling and enhanced upper-ocean warming. Although the timing of warming responses in the model is delayed compared to the observations, the experiments effectively demonstrate how SSSAs influence MLD and SST, highlighting the significant role of SSSA in modulating MHW intensity.

4 Conclusions and discussion

In this study, we have examined the role of salinity in the 2013–2014 MHW event in the Northeast Pacific using reanalysis data and climate model outputs. Our findings reveal a significant negative correlation between SSSAs and SSTAs during the MHW event. The SSSAs reduce the MLD in the region of the MHW, which facilitates heat accumulation in the upper ocean, thereby enhancing the MHW intensity. Notably, the salinity effect

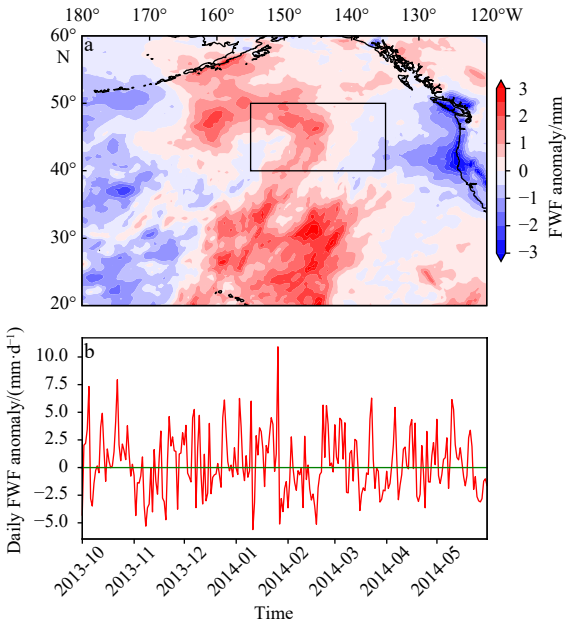

Fig. 7. Spatial distribution of mean FWF anomalies during the 2013–2014 MHW (November 21, 2013 to March 30, 2014) (a) and time series of daily FWF anomalies averaged over 40°–50°N, 135°–155°W derived from ERA5 reanalysis (b). The black box represents the region of 40°–50°N, 135°–155°W.

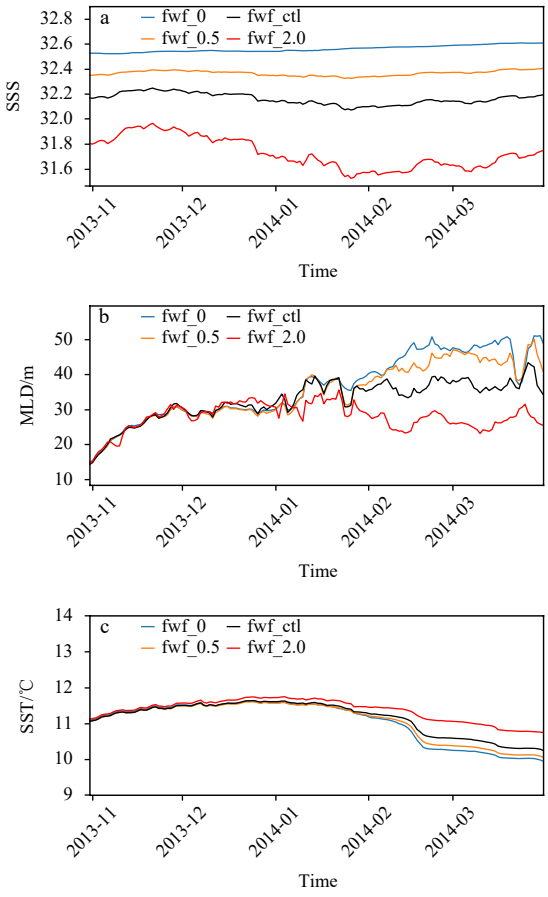

Fig. 8. Time series illustrating the results of sensitivity experiments for SSS (a), MLD (b), and SST (c). Black lines represent the results of control experiment. Blue lines represent the results of 0 precipitation. Yellow lines represent the results of halved precipitation. Red lines represent the results of doubled precipitation.

accounts for a larger portion of the negative MLD anomalies during the early stage of the MHW event compared to those induced by SSTAs. Further analysis suggests that the FWF anomalies during the MHW event significantly impact the SSSA, which is supported by model sensitivity experiments conducted using the LICOM3 model.

Previously, Zhi et al. (2019a) also examined the salinity effect on the 2013–2014 MHW in the Northeast Pacific using monthly data. In this study, we use daily data to investigate the influence of ocean salinity on shorter time scales, along with a more accurate temporal range of the 2013–2014 MHW event (November 21, 2013 to March 30, 2014). Moreover, we specifically examine the impact of FWF anomalies on the SSSA, while Zhi et al. (2019a) mainly focus on how the SSSA is driven by physical processes within the ocean interior. Our results agree with those of Zheng and Zhang (2015), who found that ENSO-related interannual salinity variability has a more pronounced impact on ocean stratification than temperature in the tropical Pacific. It is thus suggested that salinity also plays a crucial role in modulating stratification and associated processes at higher latitudes.

To validate the conclusions of this study, two additional MHW events in the Northeast Pacific have been analyzed, referred to as Event 2 (February 28–April 3, 2015) and Event 3 (May 23–July 11, 2015). Event 2 lasts 35 d with a cumulative intensity of 45.03℃ and a maximum intensity of 1.51℃. The correlation coefficient between SSTAs and SSSAs is –0.95 during Event 2, with salinity having a greater impact on MLD anomalies than temperature. Co-occurrences of positive SSTAs, negative SSSAs, and negative MLD anomalies during Event 2 are also observed in ARGO data. These results are consistent with our findings for the 2013–2014 MHW.

On the other hand, Event 3 exhibits a different relationship between SSTAs and SSSAs. This event persists for 50 d with a cumulative intensity of 73.42℃ and reached a maximum intensity of 2.08℃. Unlike Event 2, Event 3 exhibited a positive correlation between SSTA and SSSA, with temperature playing a more dominant role in driving MLD anomalies than salinity. These contrasting results highlight the complex mechanisms behind MHWs and underscore the need for further studies to better understand the salinity effect and its relation to MHWs.

While our study reveals a close connection between the SSSAs and the MHW event, the present results do not indicate a direct cause-effect relationship between SSSAs and MHWs. As shown in Fig. 3b, the SSSAs and SSTAs emerge and evolve concurrently, making it challenging to establish a clear causal relationship between these two variables. Nevertheless, it is important to note the modulation effect of salinity on MLD can be greater than temper-

ature, which is not extensively explored in many previous studies. It is worth noting that the influence of salinity on negative MLD anomalies is more pronounced during the early stage of the MHW event rather than exerting a sustained, net influence over the entire event period, which requires further investigation in future research.

This study reveals the close relationship between MHWs and ocean salinity. Our findings demonstrate that SAs significantly affect the intensity of the 2013–2014 MHW event. Therefore, it is imperative to consider the salinity effect on future MHW studies. Given the complexity of MHW dynamics, it is essential to examine the role of salinity under global warming (Schlegel et al., 2017; Zhang and Zheng, 2022). Specifically, a more comprehensive study is desired to further quantify the contributions of multiple processes, including the long-term warming trend in the Northeast Pacific (Hu et al., 2024), to the unprecedented intensity of the 2013–2014 MHW. In addition, further study is needed to clarify the sources of precipitation that cause FWF anomalies. We believe incorporating salinity as a metric for MHWs could improve forecasting efforts and deepen our understanding of their development.

Acknowledgements

We thank the anonymous reviewers for their constructive feedback that helps greatly improve the manuscript. We thank Nanjing Hurricane Translation for reviewing the English language quality of this paper.

References

Amaya D J, Miller A J, Xie S P, et al. 2020. Physical drivers of the summer 2019 North Pacific marine heatwave. Nature Communications, 11(1): 1903, doi: 10.1038/s41467-020-15820-w

Bao Qing, Liu Yimin, Wu Guoxiong, et al. 2020. CAS FGOALS-f3-H and CAS FGOALS-f3-L outputs for the high-resolution model intercomparison project simulation of CMIP6. Atmospheric and Oceanic Science Letters, 13(6): 576–581, doi: 10.1080/16742834.2020.1814675

Bond N A, Cronin M F, Freeland H, et al. 2015. Causes and impacts of the 2014 warm anomaly in the NE Pacific. Geophysical Research Letters, 42(9): 3414–3420, doi: 10.1002/2015GL063306

Bosc C, Delcroix T, Maes C. 2009. Barrier layer variability in the western Pacific warm pool from 2000 to 2007. Journal of Geophysical Research: Oceans, 114(C6): C06023

Cavole L M, Demko A M, Diner R E, et al. 2016. Biological impacts of the 2013–2015 warm-water anomaly in the Northeast Pacific: winners, losers, and the future. Oceanography, 29(2): 273–285

Chen Huanhuan, Wang Yuntao, Xiu Peng, et al. 2023. Combined oceanic and atmospheric forcing of the 2013/14 marine heatwave in the northeast Pacific. npj Climate and Atmospheric Science, 6(1): 3, doi: 10.1038/s41612-023-00327-0

Cheng Yangyan, Zhang Min, Song Zhenya, et al. 2023. A quantitative analysis of marine heatwaves in response to rising sea surface temperature. Science of the Total Environment, 881: 163396, doi: 10.1016/j.scitotenv.2023.163396

Da-Allada C Y, Penhoat Y D, Jouanno J, et al. 2014. Modeled mixed-layer salinity balance in the Gulf of Guinea: Seasonal and interannual variability. Ocean Dynamics, 64(12): 1783–1802, doi: 10.1007/s10236-014-0775-9

de Boyer Montégut C, Madec G, Fischer A S, et al. 2004. Mixed layer depth over the global ocean: An examination of profile data and a profile-based climatology. Journal of Geophysical Research: Oceans, 109(C12): C12003

Delcroix T, Cravatte S, McPhaden M J. 2007. Decadal variations and trends in tropical Pacific sea surface salinity since 1970. Journal of Geophysical Research: Oceans, 112(C3): C03012

Guan Cong, Tian Feng, McPhaden M J, et al. 2023. Zonal structure of tropical pacific surface salinity anomalies affects the eastern and central Pacific El Niños differently. Geophysical Research Letters, 50(21): e2023GL105554

Gupta A S, Thomsen M, Benthuysen J A, et al. 2020. Drivers and impacts of the most extreme marine heatwave events. Scientific Reports, 10(1): 19359

Hasson A E A, Delcroix T, Dussin R. 2013. An assessment of the mixed layer salinity budget in the tropical Pacific Ocean. Observations and modelling (1990–2009). Ocean Dynamics, 63(2−3): 179–194

Hersbach H, Bell B, Berrisford P, et al. 2018. ERA5 hourly data on single levels from 1940 to present. Copernicus Climate Change Service (C3S) Climate Data Store (CDS), https://doi.org/10.24381/cds.adbb2d47[2018-06-14/2023-04-10]

Hobday A J, Alexander L V, Perkins S E, et al. 2016. A hierarchical approach to defining marine heatwaves. Progress in Oceanography, 141: 227–238, doi: 10.1016/j.pocean.2015.12.014

Holbrook N J, Gupta A S, Oliver E C J, et al. 2020. Keeping pace with marine heatwaves. Nature Reviews Earth & Environment, 1(9): 482–493

Holbrook N J, Scannell H A, Gupta A S, et al. 2019. A global assessment of marine heatwaves and their drivers. Nature Communications, 10(1): 2624, doi: 10.1038/s41467-019-10206-z

Hu Zengzhen, Kumar A, Jha B, et al. 2017. Persistence and predictions of the remarkable warm anomaly in the northeastern Pacific Ocean during 2014–16. Journal of Climate, 30(2): 689–702, doi: 10.1175/JCLI-D-16-0348.1

Hu Shijian, Li Shihan. 2022. Progress and prospect of marine heatwave study. Advances in Earth Science (in Chinese), 37(1): 51–64

Hu Zengzhen, Mcphaden M J, Huang Boyin, et al. 2024. Accelerated warming in the North Pacific since 2013. Nature Climate Change, 14(9): 929–931, doi: 10.1038/s41558-024-02088-x

Hu Shijian, Sprintall J. 2016. Interannual variability of the Indonesian Throughflow: The salinity effect. Journal of Geophysical Research: Oceans, 121(4): 2596–2615, doi: 10.1002/2015JC011495

Huang Boyin, Liu Chunying, Banzon V, et al. 2021. Improvements of the daily optimum interpolation sea surface temperature (DOISST) version 2.1. Journal of Climate, 34(8): 2923–2939, doi: 10.1175/JCLI-D-20-0166.1

Huang Boyin, Mehta V M. 2004. Response of the Indo-Pacific warm pool to interannual variations in net atmospheric freshwater. Journal of Geophysical Research: Oceans, 109(C6): C06022

Huang Boyin, Mehta V M, Schneider N. 2005. Oceanic response to idealized net atmospheric freshwater in the Pacific at the decadal time scale. Journal of Physical Oceanography, 35(12): 2467–2486, doi: 10.1175/JPO2820.1

Jouanno J, Marin F, Penhoat Y D, et al. 2011. Seasonal heat balance in the upper 100 m of the equatorial Atlantic Ocean. Journal of Geophysical Research: Oceans, 116(C9): C09003

Kara A B, Rochford P A, Hurlburt H E. 2000. An optimal definition for ocean mixed layer depth. Journal of Geophysical Research: Oceans, 105(C7): 16803–16821, doi: 10.1029/2000JC900072

Kintisch E. 2015. 'The Blob' invades Pacific, flummoxing climate experts. Science, 348(6230): 17–18, doi: 10.1126/science.348.6230.17

Li Kexin, Zheng Fei. 2022. Effects of a freshening trend on upper-ocean stratification over the central tropical Pacific and their representation by CMIP6 models. Deep-Sea Research Part Ⅱ: Topical Studies in Oceanography, 195: 104999, doi: 10.1016/j.dsr2.2021.104999

Lin Pengfei, Yu Zhipeng, Liu Hailong, et al. 2020. LICOM model datasets for the CMIP6 ocean model intercomparison project. Advances in Atmospheric Sciences, 37(3): 239–249, doi: 10.1007/s00376-019-9208-5

Liu Hailong, Lin Pengfei, Yu Yongqiang, et al. 2012. The baseline evaluation of LASG/IAP Climate System Ocean Model (LICOM) version 2. Acta Meteorologica Sinica, 26(3): 318–329, doi: 10.1007/s13351-012-0305-y

Lukas R, Lindstrom E. 1991. The mixed layer of the western equatorial Pacific Ocean. Journal of Geophysical Research: Ocean, 96(S01): 3343–3357, doi: 10.1029/90JC01951

Maes C, Picaut J, Belamari S. 2005. Importance of the salinity barrier layer for the buildup of El Niño. Journal of Climate, 18(1): 104–118, doi: 10.1175/JCLI-3214.1

Manabe S, Stouffer R J. 1995. Simulation of abrupt climate change induced by freshwater input to the North Atlantic Ocean. Nature, 378(6553): 165–167, doi: 10.1038/378165a0

Miao Yuqing, Xu Haiming, Liu Jiawei. 2021. Variation of summer marine heatwaves in the Northwest Pacific and associated air-sea interaction. Journal of Tropical Oceanography (in Chinese), 40(1): 31–43

Miller J R. 1976. The salinity effect in a mixed layer ocean model. Journal of Physical Oceanography, 6(1): 29–35, doi: 10.1175/1520-0485(1976)006<0029:TSEIAM>2.0.CO;2>

Oka A, Hasumi H. 2004. Effects of freshwater forcing on the Atlantic deep circulation: a study with an OGCM forced by two different surface freshwater flux datasets. Journal of Climate, 17(11): 2180–2194, doi: 10.1175/1520-0442(2004)017<2180:EOFFOT>2.0.CO;2

Oliver E C J, Benthuysen J A, Bindoff N L, et al. 2017. The unprecedented 2015/16 Tasman Sea marine heatwave. Nature Communications, 8(1): 16101, doi: 10.1038/ncomms16101

Oliver E C J, Benthuysen J A, Darmaraki S, et al. 2021. Marine heatwaves. Annual Review of Marine Science, 13: 313–342, doi: 10.1146/annurev-marine-032720-095144

Oliver E C J, Donat M G, Burrows M T, et al. 2018. Longer and more frequent marine heatwaves over the past century. Nature Communications, 9(1): 1324, doi: 10.1038/s41467-018-03732-9

Pearce A, Lenanton R, Jackson G, et al. 2011. The "marine heat wave" off Western Australia during the summer of 2010/11. In: Fisheries Research Report No. 222. Western Australia: Department of Fisheries, 40

Reynolds R W, Smith T M, Liu Chunying, et al. 2007. Daily high-resolution-blended analyses for sea surface temperature. Journal of Climate, 20(22): 5473–5496, doi: 10.1175/2007JCLI1824.1

Scannell H A, Johnson G C, Thompson L, et al. 2020. Subsurface evolution and persistence of marine heatwaves in the Northeast Pacific. Geophysical Research Letters, 47(23): e2020GL090548, doi: 10.1029/2020GL090548

Scannell H A, Pershing A J, Alexander M A, et al. 2016. Frequency of marine heatwaves in the North Atlantic and North Pacific since 1950. Geophysical Research Letters, 43(5): 2069–2076, doi: 10.1002/2015GL067308

Schlegel R W, Oliver E C J, Perkins-Kirkpatrick S, et al. 2017. Predominant atmospheric and oceanic patterns during coastal marine heatwaves. Frontiers in Marine Science, 4: 323, doi: 10.3389/fmars.2017.00323

Shi Jian, Tang Cong, Liu Qinyu, et al. 2022. Role of mixed layer depth in the location and development of the Northeast Pacific warm blobs. Geophysical Research Letters, 49(16): e2022GL098849, doi: 10.1029/2022GL098849

Smale D A, Wernberg T, Oliver E C J, et al. 2019. Marine heatwaves threaten global biodiversity and the provision of ecosystem services. Nature Climate Change, 9(4): 306–312, doi: 10.1038/s41558-019-0412-1

Song S Y, Yeh S W, Kim H, et al. 2023. Arctic warming contributes to increase in Northeast Pacific marine heatwave days over the past decades. Communications Earth & Environment, 4(1): 25

Sprintall J, Tomczak M. 1992. Evidence of the barrier layer in the surface layer of the tropics. Journal of Geophysical Research: Oceans, 97(C5): 7305–7316, doi: 10.1029/92JC00407

Viglione G. 2021. How heatwaves ravage the seas. Nature, 593(7857): 26–28, doi: 10.1038/d41586-021-01142-4

Vinogradova N T, Ponte R M. 2013. Clarifying the link between surface salinity and freshwater fluxes on monthly to interannual time scales. Journal of Geophysical Research: Oceans, 118(6): 3190–3201, doi: 10.1002/jgrc.20200

Wang Aimei, Wang Hui, Fan Wenjing, et al. 2021. Study on characteristics of marine heatwave in the China offshore in 2019. Haiyang Xuebao (in Chinese), 43(6): 35–44

Ye Shuoni, Zhang Ronghua, Wang Hongna. 2023. The role played by tropical cyclones-induced freshwater flux forcing in the upper-ocean responses: A case for Typhoon Yutu (2018). Ocean Modelling, 184: 102211, doi: 10.1016/j.ocemod.2023.102211

Yu Zipeng, Lin Pengfei, Liu Hailong, et al. 2019. Short commentary on CMIP6 Ocean Model Intercomparison Project (OMIP). Climate Change Research (in Chinese), 15(5): 503–509

Zhang Ronghua, Busalacchi A J. 2009. Freshwater flux (FWF)-induced oceanic feedback in a hybrid coupled model of the tropical Pacific. Journal of Climate, 22(4): 853–879, doi: 10.1175/2008JCLI2543.1

Zhang Ronghua, Busalacchi A J, Murtugudde R G, et al. 2006. An empirical parameterization for the salinity of subsurface water entrained into the ocean mixed layer (S_e) in the tropical Pacific. Geophysical Research Letters, 33(2): L02605

Zhang Ronghua, Kleeman R, Zebiak S E, et al. 2005. An empirical parameterization of subsurface entrainment temperature for improved SST anomaly simulations in an intermediate ocean model. Journal of Climate, 18(2): 350–371, doi: 10.1175/JCLI-3271.1

Zhang Ronghua, Wang Guihua, Chen Dake, et al. 2010. Interannual biases induced by freshwater flux and coupled feedback in the tropical Pacific. Monthly Weather Review, 138(5): 1715–1737, doi: 10.1175/2009MWR3054.1

Zhang Xiaojuan, Zheng Fei. 2022. Analysis of multi-time scale variation characteristics and climate regulation factors on global marine heatwaves. Climatic and Environmental Research (in Chinese), 27(1): 170–182

Zhang Wenjing, Zheng Zhaoyong, Zhang Ting, et al. 2020. Strengthened marine heatwaves over the Beibu Gulf coral reef regions from 1960 to 2017. Haiyang Xuebao (in Chinese), 42(5): 41–48

Zhang Ronghua, Zheng Fei, Zhu Jieshun, et al. 2012. Modulation of El Niño-Southern Oscillation by freshwater flux and salinity variability in the tropical Pacific. Advances in Atmospheric Sciences, 29(4): 647–660, doi: 10.1007/s00376-012-1235-4

Zheng Fei, Zhang Ronghua. 2012. Effects of interannual salinity variability and freshwater flux forcing on the development of the 2007/08 La Niña event diagnosed from Argo and satellite data. Dynamics of Atmospheres and Oceans, 57: 45–57, doi: 10.1016/j.dynatmoce.2012.06.002

Zheng Fei, Zhang Ronghua. 2015. Interannually varying salinity effects on ENSO in the tropical Pacific: A diagnostic analysis from Argo. Ocean Dynamics, 65(5): 691–705, doi: 10.1007/s10236-015-0829-7

Zheng Fei, Zhang Ronghua, Zhu Jiang. 2014. Effects of interannual salinity variability on the barrier layer in the western-central equatorial Pacific: A diagnostic analysis from Argo. Advances in Atmospheric Sciences, 31(3): 532–542, doi: 10.1007/s00376-013-3061-8

Zhi Hai, Lin Pengfei, Zhang Ronghua, et al. 2019a. Salinity effects on the 2014 warm "Blob" in the Northeast Pacific. Acta Oceanologica Sinica, 38(9): 24–34, doi: 10.1007/s13131-019-1450-2

Zhi Hai, Zhang Ronghua, Lin Pengfei, et al. 2015. Simulation of salinity variability and the related freshwater flux forcing in the tropical Pacific: An evaluation using the Beijing Normal University Earth System Model (BNU-ESM). Advances in Atmospheric Sciences, 32(11): 1551–1564, doi: 10.1007/s00376-015-4240-6

Zhi Hai, Zhang Ronghua, Lin Pengfei, et al. 2019b. Interannual salinity variability in the tropical Pacific in CMIP5 simulations. Advances in Atmospheric Sciences, 36(4): 378–396, doi: 10.1007/s00376-018-7309-1

Zhu Jieshun, Huang Bohua, Zhang Ronghua, et al. 2014. Salinity anomaly as a trigger for ENSO events. Scientific Reports, 4(1): 6821, doi: 10.1038/srep06821